Behavior of FRP confined ultrahigh-strength concrete columns under axial compression: An experimental study

S. Jiang, D. Fernando & J.C.M. Ho
School of Civil Engineering, The University of Queensland, St Lucia, Australia

M. Heitzmann
School of Mechanical and Mining Engineering, The University of Queensland, St Lucia, Australia

ABSTRACT: Ultra High-Strength Concrete (UHSC) have become increasingly popular within the civil engineering community. While many studies exist on structural members made using UHSC, research works on the behavior of Fiber Reinforced Polymer (FRP)-confined UHSC columns are scarce. Existing theoretical models for predicting the behavior of FRP-confined normal strength and high strength concrete found to be inadequate for FRP-confined UHSC with silica fume. Due to inconstancies of existing limited experimental results on FRP-confined UHSC columns, effect of silica fume cannot be clearly identified. This paper presents an experimental study on the compressive performance of twelve FRP-confined UHSC columns under axial compression. The variables investigated include unconfined concrete strength (two different mix designs with different silica fume content) and number of GFRP plies. While GFRP confinement significantly enhance both compressive strength and ultimate strain, effectiveness of GFRP confinement was found to be largely effected by the concrete mix design.

1 INTRODUCTION

Retrofitting of concrete columns using Fibre-Reinforced Polymer (FRP) jackets with fibres predominately oriented in the hoop direction has become popular within the structural engineering community. FRP-confinement could increase both the compressive strength and ultimate strain of concrete columns (Jiang and Teng 2007; Lim and Ozbakkaloglu 2013). While, many studies have been conducted on the behaviour of FRP-confined Normal Strength Concrete (NSC) (i.e. compressive strength less than 50 MPa) columns, only few studies have been conducted on studying the behaviour of FRP-confined High-Strength Concrete (HSC) (i.e. compressive strength over 50 MPa) columns, and even fewer studies on FRP-confined Ultra-High Strength Concrete (UHSC) (i.e. compressive strength 80 MPa) columns. It is widely accepted that HSC structural members generally behaves differently to those of NSC (e.g. HSC demonstrate more brittle failure process). Nevertheless, Xiao et al. (2010) showed that the axial stress-strain model of Jiang and Teng (2007) initially developed for NSC, is also accurate for FRP-confined HSC. However, comparisons were made only on limited experimental data, and the applicability of the model on a wider test database was not confirmed. Lim and Ozbakkaloglu (2013) proposed

a new model to predict the stress-strain behaviour of FRP-confined HSC. The proposed model was validated using a database of 231 tests from 23 sources. In such comparisons however, no attention was paid to the influence of mineral admixtures used in making HSC, especially silica fume content. The test results from FRP-confined HSC with silica fume were excluded from the database of Lim and Ozbakkaloglu (2013). Setunge et al. (1993) found from tri-axial tests that silica fume had a significant effect on the behaviour of confined HSC. As HSC with and without silica fume may have different lateral expansion properties, behaviour of FRP-confined HSC with and without silica fume is expected to be different. Xiao et al. (2010) compared the axial stress-axial strain predictions from Jiang and Teng's (2007) model with the experimental results reported by Berthet et al. (2005) on FRP-co fined concrete columns with silica fume. Jiang and Teng (2007) model was found to considerably overestimate the axial stress-axial strain response. Due to inconsistencies of the existing test results (Ansari and Li 1998; Xie et al. 1995; Attard and Sethunge 1996), it is difficult to quantify the effect of additional admixtures on confinement effectiveness.

In this paper, 12 Glass FRP (GFRP)-confined UHSC short columns with silica fume were tested under axial compression. Investigated variables

include unconfined concrete strength and the number of GFRP layers.

2 EXPERIMENTAL PROGRAM

2.1 Material properties and specimen preparation

In total 12 specimens were tested, covering two different GFRP thicknesses and two different concrete mixes. Two concrete mixes (named batch A and batch B) used in this study were aimed at 28 days cylinder compressive strength of 100 MPa and 120 MPa respectively. The mix design of each batch is given in Table 1.

For each GFRP tube thickness, 6 GFRP tubes were fabricated with 3 for batch A concrete and 3 for batch B concrete. The GFRP tubes were manufactured using wet lay-up technique, by wrapping unidirectional GFRP woven fabric around a 110 mm external diameter PVC pipe. The fiber direction of GFRP was oriented along the hoop direction. Overlapping zone of half circumferential distance, i.e. 173 mm was provided. Tubes in length of 1.2 m were fabricated and once adhesive is cured, cut in to six 200 mm long tubes. Once all the tubes were prepared, casting of the concrete was carried out. Three nominally identical specimens were manufactured for each combination of concrete mix and the number of GFRP layers. In order to prevent local failure of FRP at both ends of specimen, three additional layers of 20 mm width GFRP cap was applied.

Each specimen was given a unique three-digit name (see Table 2). First digit consists of a letter (i.e. "A" or "B") to represent the concrete mix. Second digit represents the number of GFRP layers (i.e. 4 or 6). The third and final digit is given a roman number I, II, or III to differentiate between the three nominally identical specimens. For example, A-4-I is the first specimen of a four-ply GFRP tube and batch A concrete.

Table 1. Mix designs for concrete batches A and B (kg/m³).

Ingredients	Batch	
	A	B
Cement	424.7	396.1
Fly ash	158.4	198.9
Silica fume	49.4	69.2
Water	157.3	133
Coarse sands	324	324
Manufactured sands	324	324
Coarse aggregate	1044	1044
Superplasticizer	19.1	26.8

2.2 Material properties

Tensile test of five FRP flat coupons were conducted, according to the ASTM Standard (D3039/3039M-10) to obtain GFRP mechanical properties. Average tensile strength in the fibre direction was found to be 834 MPa, while tensile elastic modulus in the fibre direction was found to be 34GPa.

Three plain concrete cylinders of 100 mm in diameter and 200 mm in height were tested under axial compression to determine the properties of the concrete in each batch. The compressive strength and compressive strain at peak stress of the concrete averaged from the concrete cylinder tests are also given in Table 2. Testing of the pure cylinders as well as the FRP confined cylinders were done within 28+/-2 days from the original casting date of concrete.

Table 2. Details of the specimens.

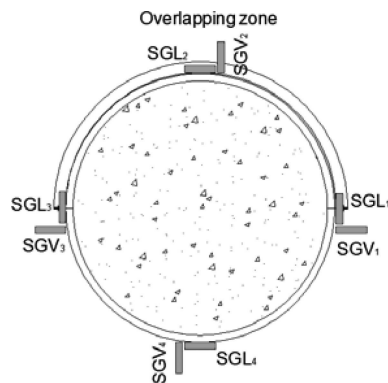| Specimen	Diameter of the concrete cylinder (mm)	No of FRP plies	Unconfined concrete strength (MPa)	Strain corresponding to unconfined concrete strength
A-4-1	110	4	104.5	0.0023
A-4-2				
A-4-3				
A-6-1		6		
A-6-2				
A-6-3				
B-4-1		4		
B-4-2			107.7	0.0017
B-4-3				
B-6-1		6		
B-6-2				
B-6-3				

Figure 1. Layout of the strain gauges.

1738

## 2.3 Instrumentation and testing

For each specimen, eight unidirectional strain gauges, 4 in longitudinal direction (SGV in Figure 1) and 4 in hoop direction (SGL in Figure 1) were installed at the mid height of the. All specimens were tested under uniaxial compression using a 3 MN capacity TechnoTest compression machine 28 days after concrete casting. Load was applied at a stress rate of 0.33 MPa/s until failure. The load and axial shortening measurements were taken directly from the loading machine.

3 EXPERIMENTAL RESULTS AND DISCUSSION

3.1 General

All the FRP-confined specimens failed due to the hoop tensile rupture of the FRP jacket (Figure 2a) with a sudden explosive noise. FRP rupture generally occurred outside the overlapping zones. Few specimens also showed limited delamination of GFRP plies at the end of overlapping zone (Figure 2b). Such delamination could not be seen outside the overlapping zone. The key test results including the hoop rupture strain of the FRP jacket $\varepsilon_{h,rup}$, the ultimate axial strain ε_{cu}, the axial stress at ultimate axial strain f'_{cu}, are summarized in Table 3.

For specimens with 4-ply GFRP, average compressive strength increase was found to be 193% for batch A concrete and 181% for batch B concrete. For specimens with 6-ply GFRP, average compressive strength increase was 259% for batch A concrete and 226% for batch B concrete. In terms
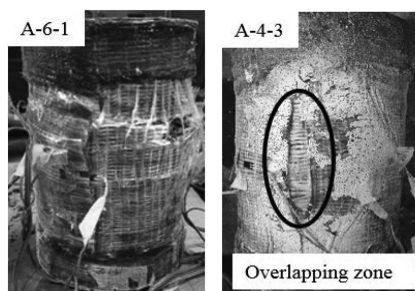
(a) GFRP rupture failure   (b)Delamination at the end of overlapping

Figure 2. Typical failure modes of the specimens.

of the compressive strength enhancement, GFRP confinement was found to be more effective for batch A concrete than for batch B concrete. However, in terms of the axial ultimate strain, for specimens with 4-ply GFRP, batch A specimens showed 587% increase in strain while batch B specimens showed 776% increase in ultimate strain. For specimens with 6-ply GFRP, batch A concrete showed 509% increase in strain capacity while batch B showed 594% increase in strain capacity. Therefore, in terms of ultimate strain, GFRP confinement had a higher influence on batch B concrete. For both batch A and batch B concrete, confined compressive strength increased, while the ultimate strain reduced with the number of GFRP plies. Lateral strain at FRP rupture was shown to be smaller for specimens with 4–ply GFRP than the specimens with 6-ply GFRP. It was also seen that

Table 3. Test results of the CSP specimens.

Specimen	P_c (kN)	Average P_c (kN)	f'_{cu} (MPa)	Average f'_{cu} (MPa)	f'_{cu}/f_{co}	ε_{cu}	Average ε_{cu}	$\varepsilon_{cu}/\varepsilon_{co}$	$\varepsilon_{h,rup}$	Average $\varepsilon_{h,rup}$
A-4-1	1809	1914	190.4	201.4	1.93	0.0133	0.0135	5.87	0.011	0.0109
A-4-2	2042		214.9			0.0117			0.0105	
A-4-3	1889		198.8			0.0154			0.0113	
A-6-1	2661	2571	280.0	270.5	2.59	0.0119	0.0117	5.09	0.0148	0.0135
A-6-2	2443		257.1			0.0118			0.0119	
A-6-3	2607		274.3			0.0115			0.0137	
B-4-1	1770	1856	186.2	195.3	1.81	0.0133	0.0132	7.76	0.0083	0.0094
B-4-2	1788		188.1			0.0158			0.0115	
B-4-3	2011		211.6			0.0104			0.0085	
B-6-1	2453	2312	258.1	243.3	2.26	0.0114	0.0101	5.94	0.0126	0.0119
B-6-2	2185		229.9			0.0083			0.0113	
B-6-3	2298		241.8			0.0106			0.0117	

P_c-ultimate axial load; f'_{cu}-confined compressive strength; f_{co}-unconfined concrete compressive strength; ε_{co}-strain at unconfined concrete compressive strength; ε_{cu}-ultimate axil strain of concrete; $\varepsilon_{h,rup}$-FRP rupture strain.

lateral strain measurements from SGL_1-SGL_4 for each specimen showed significant scatter. This will be further discussed in the next section.

3.2 *Axial stress-strain response*

The experimental axial stress-axial strain and axial stress-lateral strain curves of GFRP-confined UHSC columns are shown in Figure 3. It should be noted that axial and lateral strains of each specimen are the average values of four strain gauge readings. Similar to FRP confined NSC and HSC, the axial stress-axial strain response of GFRP-confined UHSC concrete column demonstrated an approximate bi-linear shape (Figure 3). For FRP confined NSC and HSC, the starting point of the second portion of the curve is taken as unconfined concrete strength, f_{co}. However, for batch A concrete specimens in the current study, the starting point of the second portion of the curve was found to be approximately at $1.3 f_{co}$. For batch B concrete specimens with 4-ply GFRP, initiation of the second portion of the curve was at approximately $1.3 f_{co}$, while for 6-ply GFRP specimens this initiation point was at approximately $1.5 f_{co}$. The gradient of the second portion of the curve increased with the
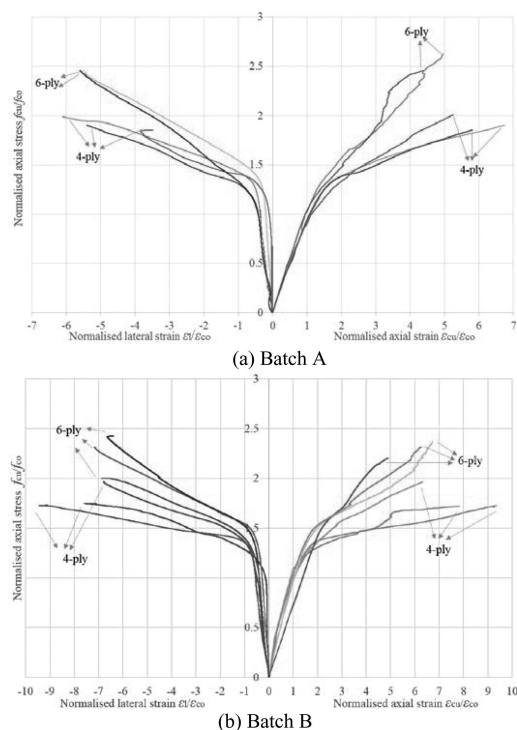
number of GFRP plies. Gradient of the second portion of the curve, for same number of GFRP plies was higher for batch A specimens compared to that of batch B specimens.

Lateral strain at ultimate load showed significant scatter between specimens. The lateral strains of each specimen plotted in Figure 3 are the average strains taken from 4 lateral strain gauges of the specimen. Axial stress-lateral strain curves from each strain gauge for several representative specimens are given in Figure 4. It can be seen that the
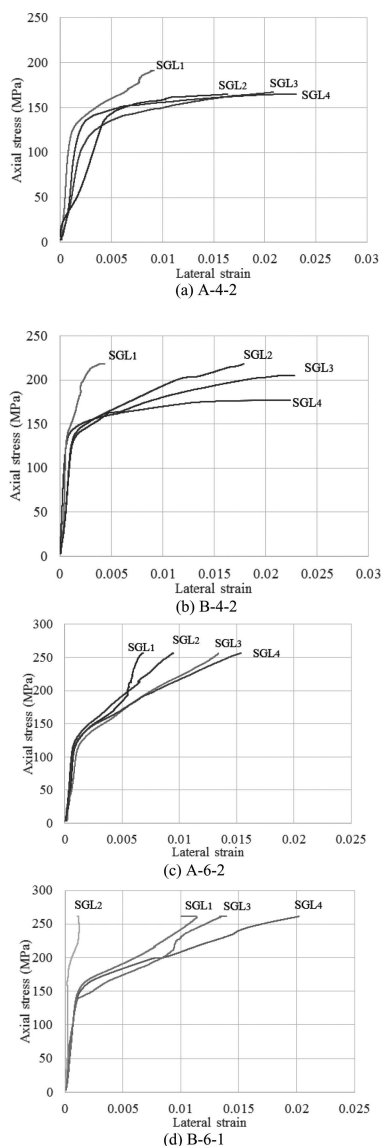

(a) A-4-2

(b) B-4-2

(c) A-6-2

(d) B-6-1

Figure 4. Axial stress-lateral strain response of selected specimens.

(a) Batch A

(b) Batch B

Figure 3. Normalized axial stress-axial strain and axial stress-lateral strain curves.

1740

axial stress-lateral strain curves are approximately of bi-linear shape. After the transition in to the second portion of the curve, strain reading close to free end of GFRP (i.e. SGL_1) deviated significantly from remaining readings. This is believed to be due to possible interfacial slip between the plies closer to the free end of the GFRP, which may result in strain relaxation. However, such slips are only limited to outermost layer of GFRP within a small region closer to the free end.

Strain readings were non-uniform around the circumference. Strain readings from SGL_2, which is within the overlapping zone showed consistently lower readings compared to strain readings from SGL_4, which is outside the overlapping zone. Similar observations were also made by number of other researchers (Shahawy et al. 2000; Xiao and Wu 2000; De Lorenzis and Tepfers 2003; Lam and Teng 2004). Lam and Teng (2003) attributed this lower strain in overlapping area to the thicker FRP tube in overlapping zone. If there are no interfacial slips between the GFRP plies, then for the same confinement pressure, the strain in the jacket is inversely proportional to the thickness of the jacket. For most of the specimens, ratio of the strain readings from SGL_2 and SGL_4 was approximately constant.

It should also be noted that, inhomogeneity of the bond resulting from wet lay-up manufacturing process may also contribute towards lateral strain variations along the circumference.

Above presented results clearly showed that the concrete mix-design had a significant effect on the behavior of the GFRP confined concrete cylinders. However, due to inconsistent results on unconfined behavior of UHSC with silica fume, and limited data available on FRP-confined UHSC with silica fume, it is difficult to identify the exact effects of silica fume on GFRP-confined UHSC behavior. Further investigations are necessary to better understand the effects of silica fume on GFRP-confined UHSC columns.

4 CONCLUSIONS

This paper presents an investigation into the behaviour of GFRP-confined UHSC columns under axial compression. Effect of silica fume was investigated through two different concrete mix designs. Effect of the number of GFRP plies was also investigated. Following observations were made from the experimental results:

1. All GFRP-confined UHSC columns failed due to rupture of GFRP with few specimens also indicating delamination of GFRP at the end of overlapping zone.

2. The ultimate compressive strength can be significantly enhanced by GFRP confinement. For batch A concrete, 4 plies of GFRP increased the compressive strength by 193% while 6 plies of GFRP increased the compressive strength by 259%. For batch B concrete, 4 plies of GFRP increased the compressive strength by 181%, while 6 plies of GFRP increased the compressive strength by 226%.

3. The ultimate strain can also be significantly enhanced by GFRP confinement. For batch A and batch B concrete, 4 plies of GFRP increased the ultimate strain by 587% and 776% respectively, while 6 plies of GFRP increased the strain by 509% and 594% respectively.

4. Silica fume content shown to have a significant influence on the behaviour of GFRP confined UHSC. While ultimate strength of unconfined concrete from batch A and batch B were similar, GFRP confined from batch A and batch B concrete showed significantly different results.

While this study confirms the effect of silica fume on the behaviour of GFRP-confined UHSC, much more work needed to better understand the behaviour of GFRP-confined UHSC.

REFERENCES

ASTM. 1992. Standard test method for apparent tensile strength of ring or tubular plastics and reinforced plastics by split disk method. D 2290-92, West Conshohocken, Pa.

ASTM. 1995. Standard test method for tensile properties of polymer matrix composite materials. D 3039/D 3039M, West Conshohocken, Pa.

ASTM. 2010. Standard test method for tensile properties of polymer matrix composite materials. D 3039/D 3039M, West Conshohocken, Pa.

Ansari, F., & Li Q. 1998. High-strength concrete subjected to triaxial compression. *ACI Materials Journal* 95(6): 747–755.

Attard, M. M., & Setunge S. 1996. Stress-strain relationship of confined and unconfined concrete. *ACI Materials Journal* 93(5).

Berthet J.F., Ferrier E. & Hamelin P. 2005. Compressive behavior of concrete externally confined by composite jackets. Part A: experimental study. *Construction and Building Materials*, 19(3): 223–232.

De Lorenzis, L., & Tepfers, R. 2003. Comparative study of models on confinement of concrete cylinders with fiber reinforced polymer composites. *J. Compos. Constr* 7(3): 219–237.

Jiang, T., & Teng J.G. 2007. Analysis-oriented stress-strain models for FRP-confined concrete. *Engineering Structures* 29(11): 2968–2986.

Lam, L., & Teng J.G. 2003. Design-oriented stress-strain model for FRP-confined concrete. *Construction and building materials* 17(6): 471–489.

Lam L., & Teng J.G. 2004. Ultimate condition of fiber reinforced polymer-confined concrete. *Journal of Composites for Construction* 8(6): 539–548.

Lim J.C., & Ozbakkaloglu T. 2013. Confinement model for FRP-confined high-strength concrete. *Journal of Composites for Construction* 18(4): 04013058.

Setunge, S., M. Attard M., & Darvall P. 1993. Ultimate strength of confined very high-strength concretes. *ACI Structural Journal*, 90(6).

Shahawy, M., Mirmiran, A., & Beitelman, A. 2000. Test and modeling of carbon-wrapped concrete columns. *Composites*, *Part B* 31: 471–480.

Xiao Q.G., Teng J.G., & Yu T. 2010. Behavior and modeling of confined high-strength concrete. *Journal of Composites for Construction*, 14(3): 249–259.

Xie, J., Elwi, A.E., & MacGregor, J.G. 1995. Mechanical properties of three high-strength concretes containing silica fume. *ACI Materials Journal* 92(2): 135–145.

Xiao, Y., & Wu, H. (2000). Compressive behavior of concrete confined by carbon fiber composite jackets. *J. Mater. Civ. Eng.*, 12(2): 139–146.

Yang X., Nanni A., & Chen G. 2001. Effect of corner radius on the performance of externally bonded FRP reinforcement. *Proc. 5th Int. Conf. on Non-Metallic Reinforcement for Concrete Structures*.